Received: 15 September 2019 | Revised: 9 December 2019 | Accepted: 10 December 2019

DOI: 10.1111/jsr.12976

REGULAR RESEARCH PAPER

Journal of Sleep Research

Targeted recombination in active populations as a new mouse genetic model to study sleep-active neuronal populations: Demonstration that Lhx6+ neurons in the ventral zona incerta are activated during paradoxical sleep hypersomnia

Hyun-Sook Lee[1,2,3] | Risa Yamazaki[1] | Dianru Wang[1] | Sébastien Arthaud[1] | Patrice Fort[1] | Laura A. DeNardo[4] | Pierre-Hervé Luppi[1]

[1]Centre de Recherche en Neurosciences de Lyon (CRNL), Université Claude Bernard Lyon 1, CNRS UMR5292, INSERM U1028, Bron, France

[2]Department of Anatomy, School of Medicine, Konkuk University, Seoul, Korea

[3]Research Institute of Medical Science, School of Medicine, Konkuk University, Seoul, Korea

[4]Department of Physiology, University of California LA, Los Angeles, CA, USA

Correspondence
Pierre-Hervé Luppi, Centre de Recherche en Neurosciences de Lyon (CRNL), Bâtiment 462-Neurocampus Michel Jouvet, 69500 Bron, France.
Email: luppi@sommeil.univ-lyon1.fr

Funding information
Universite Claude Bernard Lyon 1; The Japan Society for the Promotion of Science; Postdoctral Fellowship from the Uehara Memorial Foundation; French Embassy in Japan; Konkuk University-*14

Abstract

The cFos immunostaining allowed the identification of multiple populations of neurons involved in the generation of paradoxical sleep. We adopted the transgenic (targeted recombination in active populations) mouse model, which following injection of tamoxifen, allows expression of Cre-dependent reporter constructs (i.e., mCherry) in neurons expressing cFos during waking or paradoxical sleep hypersomnia following automatic paradoxical sleep deprivation. Three groups of mice were subjected to two periods of waking, one period of waking and one of paradoxical sleep hypersomnia, or two periods of paradoxical sleep hypersomnia. A high percentage of double-labelled neurons was observed in the lateral hypothalamic area and zona incerta of two periods of waking and two periods of paradoxical sleep hypersomnia in mice, but not in those of one period of waking and one of paradoxical sleep hypersomnia in animals. Melanin-concentrating hormone neurons in the lateral hypothalamic area and Lhx6+ cells in the zona incerta constituted 5.7 ± 1.5% and 8.8 ± 2.3% of all mCherry+ cells and 20.6 ± 4.8% and 24.6 ± 5.9% of all cFos+ neurons in two periods of paradoxical sleep hypersomnia in animals. In addition, melanin-concentrating hormone cells as well as Lhx6+ neurons rarely expressed mCherry (or cFos) in the waking condition, in contrast to orexin neurons, which constituted approximately 30% of mCherry+ and cFos+ neurons. Our results validate the TRAP methodology and open the way to use it for identifying the neurons activated during waking and paradoxical sleep hypersomnia. Furthermore, they indicate for the first time that Lhx6+ neurons in the zona incerta, like melanin-concentrating hormone cells in the lateral hypothalamic area, are activated during paradoxical sleep hypersomnia but not during waking. These results indicate that Lhx6+ neurons might play a role in the control of paradoxical sleep, like the melanin-concentrating hormone cells.

KEYWORDS

hypothalamic neuropeptides, sleep–wake cycle

H-S Lee and R. Yamazaki contributed equally.

1 | INTRODUCTION

The cFos immunostaining has long been utilized to identify the neurons activated during waking (W), slow-wave sleep (SWS) and paradoxical (i.e., rapid eye movement [REM]) sleep (PS). By this means, we and others (Blanco-Centurion et al., 2019; Varin, Luppi, & Fort, 2018; Verret et al., 2003) identified multiple populations of neurons playing a role in the generation of PS like the melanin-concentrating hormone (MCH) cells located in the lateral hypothalamic area (LHA) and zona incerta (ZI). It was later confirmed, using unit recordings, that these neurons are specifically active during PS (Hassani, Lee, & Jones, 2009) and that their opto- and chemogenetic activation induces an increase in PS quantities (Jego et al., 2013; Varin et al., 2018). These results validated the strategy of using the cFos staining to identify populations of PS-active neurons. However, the vast majority of cFos+ neurons localized in the LHA and ZI after PS hypersomnia have not been functionally characterized, although it has been shown that a large number express GAD67 and are thus GABAergic (Brown et al., 2017; Sapin, Berod, Léger, & Herman, 2010; Sapin et al., 2009). Optogenetic stimulation of GABAergic neurons in the LHA and ZI induced W rather than PS, indicating that part of these GABA neurons is W-inducing (Herrera et al., 2016). Interestingly, it has been recently reported that GABAergic neurons co-containing LIM homeobox 6 (Lhx6) in the ventral ZI express cFos at the end of the dark period or during total sleep deprivation and that their activation (or inhibition) increases (or decreases) SWS and PS quantities (Liu et al., 2017).

Although cFos immunostaining allowed the identification of neurons activated during PS in the LHA, ZI and many other structures, the identification of their role was strongly limited due to the lack of specific markers. A new genetic strategy, so-called targeted recombination in active populations (TRAP), might be an ideal choice to study these neurons (DeNardo & Luo, 2017; Guenthner, Miyamichi, Yang, Heller, & Luo, 2013). The TRAP mice have been successfully used to characterize neurons involved in sensory coding, motor behaviour, memory, valence-encoding and SWS genesis (Allen et al., 2017; DeNardo et al., 2019; Girasole et al., 2018; Tasaka et al., 2018; Zhang et al., 2019). The striking advantage of such transgenic mice is that they allow Cre-dependent reporter constructs in the neurons expressing cFos at a given time by means of injecting 4-OH-tamoxifen (4-OHT). In particular, permanent Golgi-like labelling (using mCherry as a reporter gene) of activated neurons can be obtained, which can be combined with cFos labelling if the animals were perfused right after the second stimulus occurring days (or weeks) after the first stimulus.

The aim of the present study was to validate the TRAP methodology in studying the role of LHA and ZI neurons activated during PS hypersomnia and W. To this aim, we allowed the expression of mCherry and cFos in three groups of mice. The first group was put twice (1 week apart) in an open field. It received 4-OHT after the first W period and was perfused at the end of the second W period. By this means, we were able to determine whether the same cells were labeled with mCherry and cFos. We also combined staining of both markers with that of orexin (ORX) to confirm that the labelled neurons were W-active neurons. In the second group, we performed two (1 week apart) PS deprivation-rebound (PSR) procedures, which allowed us to show whether mCherry+ neurons were expressing cFos during the second PS hypersomnia. We verified that these neurons might correspond to neurons activated during PS hypersomnia by combining mCherry and cFos labelling with MCH immunostaining. The third group of mice was first exposed to the open field and then 1 week later before perfusion exposed to PSR. Double-labelling in these mice allowed us to confirm that neurons activated during W were not activated during PS hypersomnia. We finally determined whether Lhx6+ neurons are active during W or PS hypersomnia.

2 | METHODS

2.1 | Animals

We followed EU as well as French guidelines for animal care in scientific research. The experimental protocol was approved by the research ethical committee C2EA-55 of University-Lyon 1 (No. DR2014-45). Mice were housed in groups of two before surgery and in individual barrels afterwards. Animals were maintained at 22 ± 1°C under 12 hr light/dark cycles (lights on from 08:00 to 20.00 hours) with free access to food and water. The transgenic *Fos*$^{2A\text{-}iCreER/+}$ mice (*TRAP2*, for activity-dependent genetic labelling, kindly donated by Dr Liqun Luo from Stanford University) were crossed to *R26*$^{AI14/+}$ *(AI14)* mice to obtain double heterozygous (*TRAP2*;*Ai14*, *TRAP-RED*) mice (Allen et al., 2017; DeNardo et al., 2019). Activity-dependent expression of double transgenes is described in Figure 1a. Animals at 8–12 weeks of age (n = 21; 25–30 g) were utilized and every effort was made to minimize the number of mice sacrificed (W-W, n = 3; W-PSR, n = 8; PSR-PSR, n = 10). Among them, four W-PSR (M1270, 1283, M1301 and 1361) and three PSR-PSR (M1268, 1269 and 1312) mice were selected. Criteria for inclusion for analysis were mice that exhibit at least 24% of the amount of PS during the first 30-min period during 2-hr PS hypersomnia; after perfusion, these animals did show optimal cFos and mCherry staining (Figures 1–5; Tables 1 and 2).

2.2 | Surgical procedures

A mixture of ketamine (100 mg/kg) and xylazine (10 mg/kg) was injected intraperitoneally to induce anaesthesia. Using a stereotaxic device, three electroencephalogram (EEG) electrodes were implanted: two above the frontal (1 mm lateral to midline and 2 mm anterior to bregma) and parietal (1.5 mm lateral to midline and −2 mm from bregma) cortices and the third above the cerebellum (2 mm lateral to midline and −6 mm from bregma) as reference. Electrodes for electromyogram (EMG) were inserted into neck muscles.

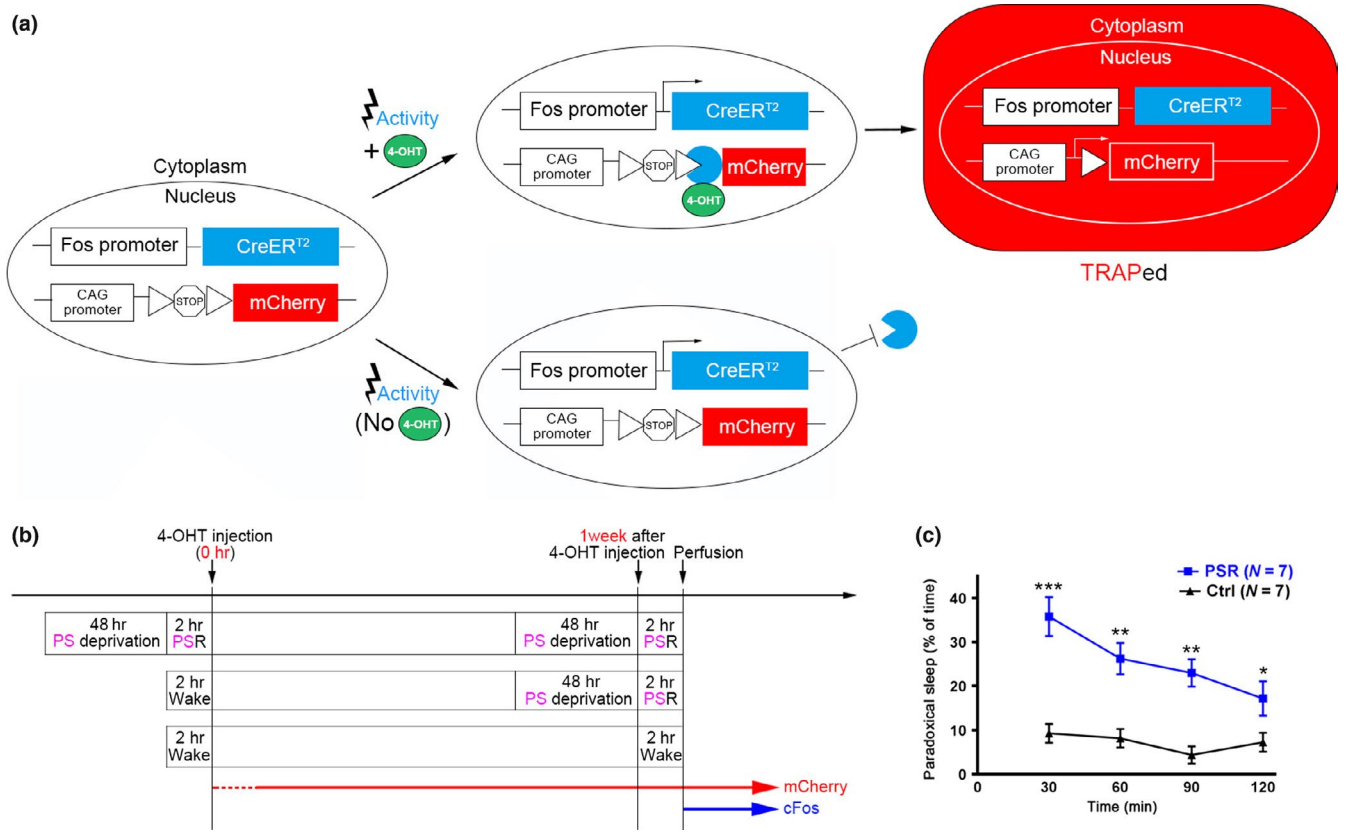

FIGURE 1 A binary (i.e., mCherry and cFos) expression system of targeted recombination in active populations (TRAP) of mice. (a) TRAP requires two transgenes: one that expresses CreER^{T2} (i.e., tamoxifen-inducible Cre recombinase) from an activity-dependent Fos promoter and the other that allows expression of an effector gene (i.e., mCherry) by means of CreER^{T2} recombination. Without 4-hydroxytamoxifen (4-OHT), CreER^{T2} (blue, pacman-shaped structure) is retained in the cytoplasm of active cells, where it is expressed, thus no recombination can occur (a, the second row). In the presence of 4-OHT, CreER^{T2} recombination (i.e., binding of CreER^{T2} into floxed alleles) can occur, inactivating the stop codon and resulting in permanent expression of mCherry (red staining, a, the first row). Non-active cells do not undergo recombination due to the absence of CreER^{T2} expression (pictures not shown). (b) Time sequence of experimental protocols for TRAPing. (c) Based on the data from Table 1, temporal evolution for the amount (%) of paradoxical sleep (PS) was represented for control (Ctrl) versus experimental states. Because the second (i.e., cFos-labelled) event was adopted from wake-PSR animals (i.e., M1270, 1283, 1301 and 1361), the corresponding second (i.e., cFos-labelled) condition was selected from PSR-PSR animals (M1268, 1269 and 1312). For statistics, the paired *t* test was employed (***$p < .001$; **$p < .01$; *$p < .05$). PSR, paradoxical sleep deprivation-rebound

2.3 | Polysomnography

Animals were allowed to recover from surgery for 1 week in their home cage before being habituated to the recording conditions for 4 days. They were connected to a cable attached to a slip-ring commutator to allow free movement within the barrel. Unipolar EEG and bipolar EMG signals were amplified (MCP-PLUS; Alpha-Omega Engineering, Israel), digitized at 512 Hz and transferred to Slip Analysis v 2.9.8 software. Vigilance states were scored using a 5-s window frame according to standard criteria (Libourel, Corneyllie, Luppi, Chouvet, & Gervasoni, 2015; Renouard et al., 2015).

2.4 | Tamoxifen injection

A stock solution (20 mg/ml) of 4-OHT (Sigma; H6278) was prepared by adding 200-proof ethanol, vortexed, and placed on a shaker at 37°C for 15 min until it dissolved. It was covered with aluminium foil to minimize light exposure. A working solution (10 mg/ml) was prepared in oil; the 4-OHT/ethanol mixture combined with corn oil (Sigma; C8267) was put into a speed-vac for 2–3 hr until ethanol evaporated. The drug was delivered intraperitoneally based on the time schedule (Figure 1b).

2.5 | Protocols for PS deprivation and rebound and W induction

Deprivation of paradoxical sleep was achieved by an automated method (Libourel et al., 2015) employing an online signal analysis with Sleepscore (Viewpoint) software. Briefly, several discriminant parameters of EEG/EMG recordings were calculated based on manual scoring of the recordings in order to automatically assign a vigilance state (W, SWS or PS) for every 1-s epoch. When a PS episode was detected, a transistor–transistor logic (TTL) signal was sent to a stimulation box through a software developed under Matlab, waking up the animal by vertical shaking of the barrel floor via an electromagnet. Automatic PS deprivation for

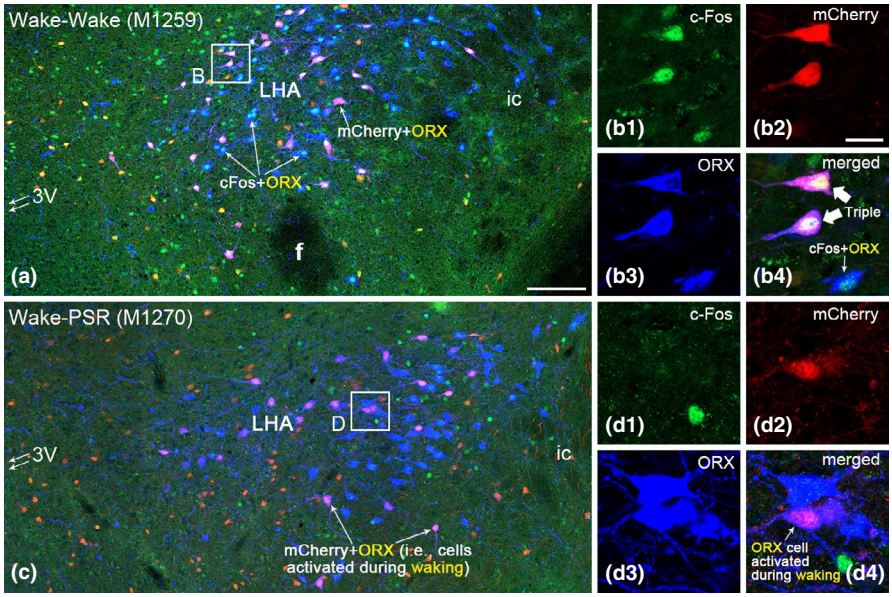

FIGURE 2 Orexin (ORX) neurons activated during wake-wake versus wake-PSR periods. In a wake-wake animal (M1259; A–B4), many mCherry+ (red) or cFos+ (green) ORX (blue) neurons were observed in the lateral hypothalamic area (LHA). In addition, triple-labelled neurons characterized by a white nucleus with violet cytoplasm were prominent (A and B4). In a wake-PSR animal (M1270; C–D4), mCherry+ (i.e., wake-active) ORX neurons were prominent, whereas cFos+ (i.e., PSR-active) ORX cells were minimal (C and D4). A and C represent tiled confocal images. 3V, third ventricle; f, fornix; ic, internal capsule; PSR, PSR, paradoxical sleep deprivation-rebound. Scale bars = 200 μm (A), 20 μm (B2)

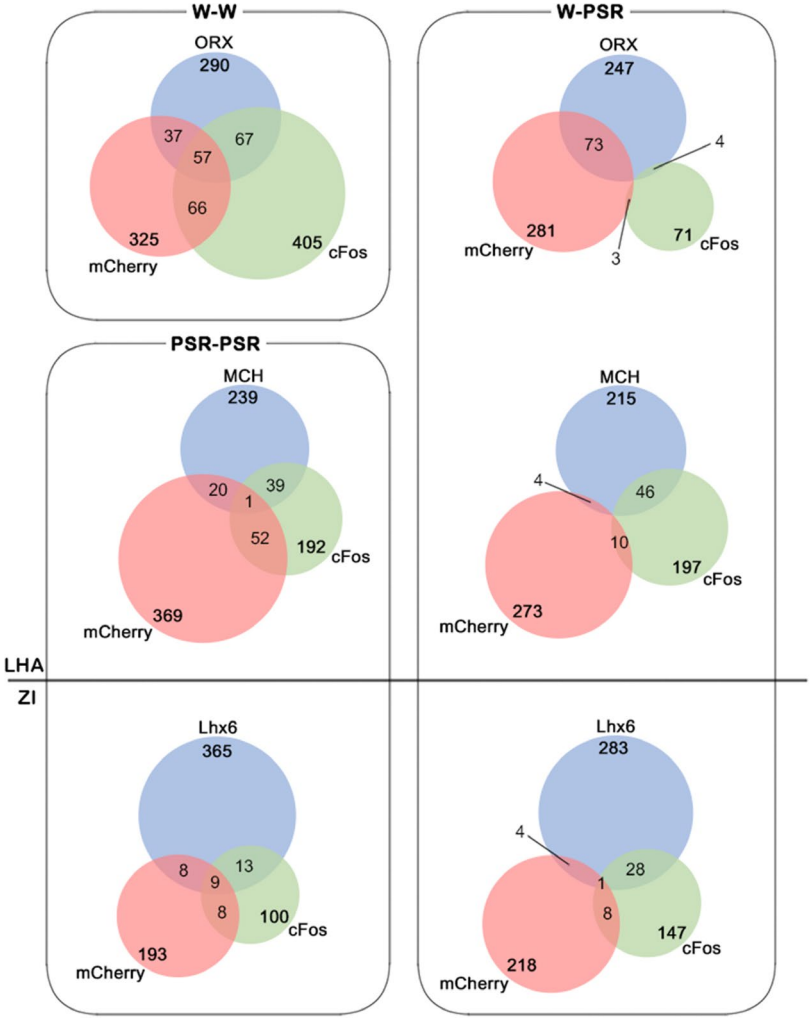

FIGURE 3 The average numbers of single-, double- or triple-labelled cells in wake-wake, wake-PSR and PSR-PSR animals are presented as Venn diagrams, whereas standard error means (*SEM*) are described in the Results section. Based on these numbers, the proportions (%) of labelled neuronal groups were calculated and statistically analysed in Table 2. PSR, paradoxical sleep deprivation-rebound. Red: mCherry, blue, Lhx6, CFos, green

48 hr was highly efficient in mice, leaving a residual amount of PS of only 2.2% (Arthaud et al., 2015). PS deprivation started at 10:00 hours, when amounts of PS are high. After 48 hr of PS deprivation, mice were returned to their home barrel, where they could sleep ad libitum during a 2-hr recovery period (Figure 1b). In PSR-PSR animals, 4-OHT was injected after 2 hr of PSR. One week later, the animals were subjected to

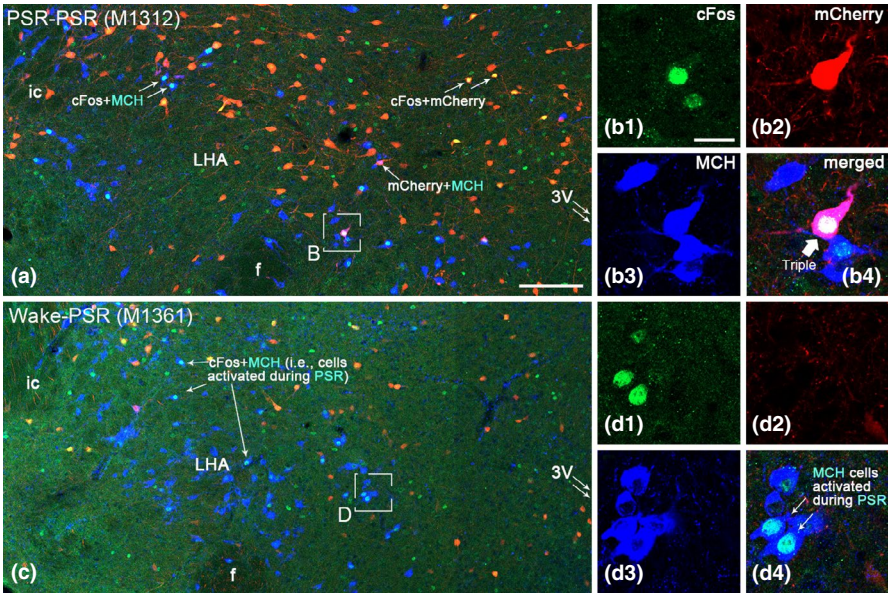

FIGURE 4 Melanin-concentrating hormone (MCH) neurons activated during PSR-PSR versus wake-PSR periods. In a PSR-PSR animal (M1312; A–B4), mCherry+ (red) as well as cFos+ (green) MCH (blue) neurons were observed in the LHA (A), whereas triple-labelled neurons characterized by a white nucleus with violet cytoplasm were rare (B4). In a wake-PSR animal (M1361; C–D4), mCherry+ (i.e., wake-active) MCH neurons were rare, but cFos+ (i.e., PSR-active) MCH cells were substantial (C and D4). A and C represent tiled confocal images. 3V, third ventricle; f, fornix; ic, internal capsule. Scale bars = 200 μm (A), 20 μm (B1). PSR, PSR, paradoxical sleep deprivation-rebound

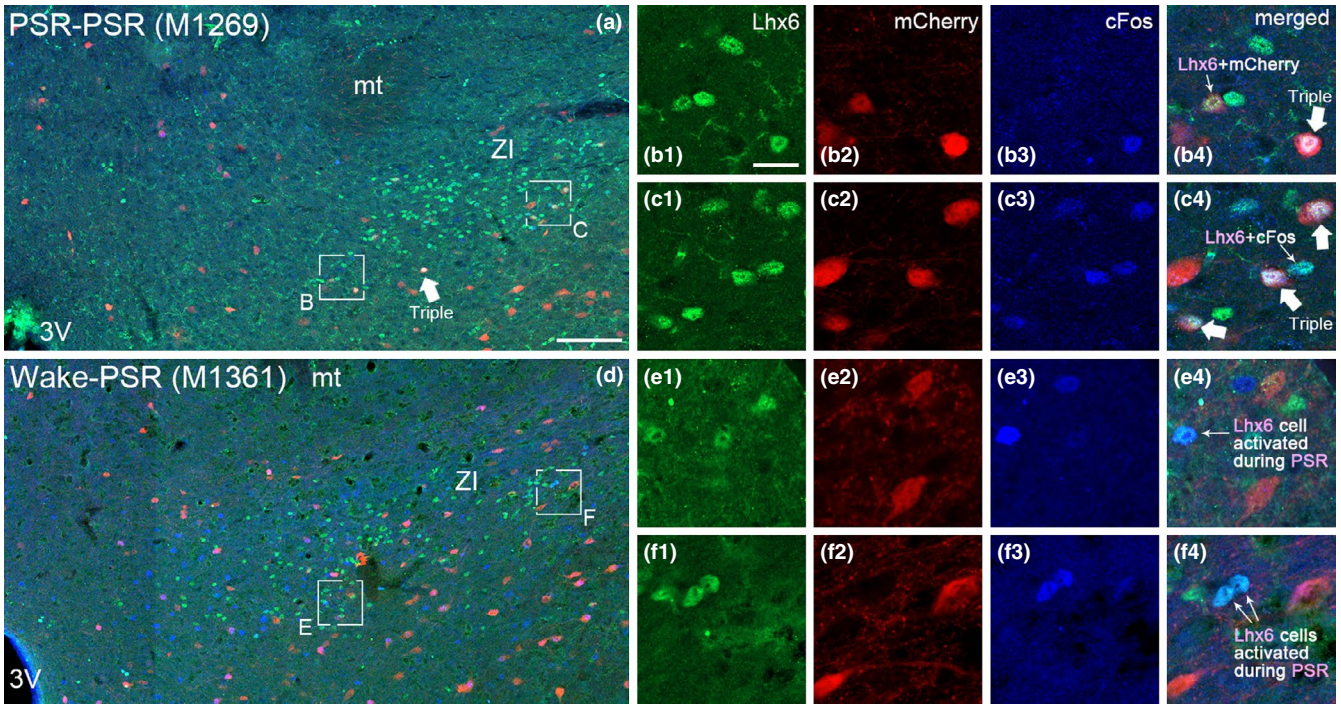

FIGURE 5 Lhx6+ neurons activated during PSR-PSR versus wake-PSR periods. In a PSR-PSR animal (M1269; A–C4), a substantial number of mCherry+ (B4, red) or cFos+ (C4, blue) Lhx6 (green) neurons was observed in the ZI. Triple-labelled neurons characterized by a white nucleus with red cytoplasm were also substantial (A, B4 and C4). In a wake-PSR animal (M1361; D–F4), a large number of cFos+ (i.e., PSR-active) Lhx6+ cells was observed (E4 and F4). A and C represent tiled confocal images. 3V, third ventricle; f, fornix; ic, internal capsule. Scale bars = 100 μm (A), 20 μm (B1). PSR, PSR, paradoxical sleep deprivation-rebound

PS deprivation and perfused after 2 hr of PSR (i.e., at noon). In W-PSR or W-W animals, mice were placed for 2 hr in a white open-field box (base, 45 × 45 cm) containing a variety of toys. The animals were monitored via video camera and polysomnography (Libourel et al., 2015). Whenever asleep, they were awakened by slow repositioning of toys or by gentle touch using a soft tissue. One week later, W-W animals were submitted to the same procedure, whereas the W-PS ones were PS deprived for 48 hr and allowed to recover for 2 hr before perfusion.

2.6 | Perfusion and cryostat sectioning

Mice were transcardially perfused with heparin-added Ringer's solution and 4% of paraformaldehyde (0.01 M phosphate-buffered saline, PBS; pH 7.4). Brains were removed and stored in 30% sucrose until they settled to the bottom. Using a cryostat, eight consecutive series of hypothalamic sections (extending from the caudal pole of the paraventricular nucleus to the rostral pole of tuberomammillary

TABLE 1 The proportion (%) of paradoxical and slow-wave sleep in wake-PSR (paradoxical sleep deprivation-rebound) versus PSR-PSR animals during 2 hr of control or PS rebound periods

Cases	Wake-PSR (*n* = 4)								PSR-PSR (*n* = 3)											
									M1268				M1269				M1312			
Animals	M1270		M1283		M1301		M1361		1st PSR		2nd PSR		1st PSR		2nd PSR		1st PSR		2nd PSR	
Sleep states	PS (%)[a]	SWS (%)[a]	PS	SWS	PS	SWS	PS	SWS	PS	SWS	PS	SWS	PS	SWS	PS	SWS	PS	SWS	PS	SWS
Control states[b]																				
0–30 min	0.00	65.57	9.44	67.77	9.73	65.83	4.72	34.73	10.83	61.67	—	—	17.78	71.67	—	—	12.22	75.27	—	—
30–60	16.94	75.00	7.22	63.03	3.07	55.57	7.50	84.70	11.39	63.33	—	—	10.83	81.93	—	—	0.00	16.10	—	—
60–90	0.28	15.00	0.00	0.83	11.10	78.07	8.33	78.87	0.00	31.93	—	—	0.56	21.13	—	—	10.00	80.57	—	—
90–120	1.11	47.50	6.39	71.93	8.07	70.57	0.00	8.9	13.89	71.97	—	—	6.39	81.67	—	—	14.72	66.10	—	—
Exp. states (i.e., PSR)																				
0–30 min	53.06	41.11	29.17	61.39	24.17	71.67	25.56	59.17	44.17	50.68	29.72	66.39	27.22	42.22	39.17	55.28	30.83	47.50	49.72	38.61
30–60	36.94	58.88	32.22	58.89	13.89	61.94	21.39	69.16	1.39	68.05	17.22	60.28	26.11	53.89	24.44	72.50	29.44	58.05	37.50	56.95
60–90	19.44	73.61	22.78	65.28	23.06	69.44	21.39	68.34	10.83	24.72	9.17	58.05	30;00	59.17	28.89	66.39	1.94	56.39	36.11	56.11
90–120	22.78	68.05	11.11	61.94	1.11	61.67	12.50	45.83	20.56	75.00	15.00	81.67	0.00	6.94	25.83	71.11	17.78	72.50	31.67	63.06

[a]The proportion (%) of PS and SWS during 2 hr of control or PS rebound periods was obtained from polysomnographic data. The proportion (%) of the wake period was omitted for simplicity, which could be easily obtained by subtracting the sum of PS and SWS from 100 (i.e., the total percentage).

[b]Control data were obtained during the same 2-hr period on the previous day before the exposure to the wake or PSR conditions); thus, the values were absent (—) in the 2nd PSR of M1268, 1269 and 1312.

TABLE 2 Activated orexin (ORX), melanin-concentrating hormone (MCH) or LIM homeobox 6 (Lhx6) neurons during wake (W)-W, W-paradoxical sleep rebound (PSR) or PSR-PSR conditions in targeted recombination in active populations (TRAP) mice

			Proportions (%)				
Peptides	Exp. conditions	Animals	Total (mCherry+ peptide+) over total mCherry	Total (mCherry+ peptide+) over total peptide	Total (cFos+ peptide+) over total cFos	Total (cFos+ peptide+) over total peptide	Triple over total peptide
ORX	W-W	M1258	39.3	25.3	31.8	34.8	13.2
		M1259	28.3	29.5	30.0	49.6	19.8
		M1363	25.6	42.0	30.4	44.3	25.7
		$\overline{X} \pm SEM$ ($n = 3$)	31.1 ± 4.2	32.3 ± 5.0	30.7 ± 0.5[a]	42.9 ± 4.3[b]	19.6 ± 3.6[c]
	W-PSR	M1270	26.9	26.9	4.3	1.9	0
		M1301	22.6	34.0	6.8	1.3	0
		M1361	30.5	28.4	7.4	1.6	0
		$\overline{X} \pm SEM$ ($n = 3$)	26.7 ± 2.3	29.8 ± 2.2	6.2 ± 0.9[a]	1.6 ± 0.2[b]	0[c]
MCH	PSR-PSR	M1268	6.4	13.0	11.0	9.5	0
		M1269	2.8	4.0	26.1	8.8	0
		M1312	7.9	10.2	24.7	31.6	1.2
		$\overline{X} \pm SEM$ ($n = 3$)	5.7 ± 1.5[d]	9.1 ± 2.7[e]	20.6 ± 4.8	16.6 ± 7.5	0.4 ± 0.4
	W-PSR	M1270	1.2	2.0	25.5	24.8	0
		M1283	1.5	1.9	24.2	19.3	0
		M1361	2.2	2.2	21.3	21.6	0
		$\overline{X} \pm SEM$ ($n = 3$)	1.6 ± 0.3[d]	2.0 ± 0.1[e]	23.7 ± 1.2	21.9 ± 1.6	0
Lhx6	PSR-PSR	M1268	6.0	4.2	35.4	5.0	2.7
		M1269	13.4	6.5	23.5	7.2	2.6
		M1312	6.9	3.0	14.9	5.4	2.4
		$\overline{X} \pm SEM$ ($n = 3$)	8.8 ± 2.3[f]	4.6 ± 1.0[g]	24.6 ± 5.9	5.9 ± 0.7[h]	2.6 ± 0.1[i]
	W-PSR	M1283	2.8	2.4	31.5	11.7	0.3
		M1301	2.0	1.6	24.7	8.4	0.4
		M1361	1.5	1.0	12.9	10.4	0.6
		$\overline{X} \pm SEM$ ($n = 3$)	2.1 ± 0.4[f]	1.7 ± 0.4[g]	23.0 ± 5.4	10.2 ± 1.0[h]	0.4 ± 0.1[i]

Note: Proportions (%) were calculated from the number of single-, double- or triple-labelled cells indicated in Figure 3. Hypothalamic sections between bregma −1.34 and −1.82 mm were obtained, where cell counts were made unilaterally using every eighth section (a total of three sections per animal; section thickness, 30 μm). Based on the Mann–Whitney *U*-test, mean difference between the two same superscripts (a–i) is statistically significant ($p < .05$).

nucleus) were obtained at the thickness of 30 μm; thus each well contained a series of 240 μm-apart sections.

2.7 | Immunofluorescence

Sections were washed with PBS containing 0.3% Triton X-100 (PBST) and then incubated in 10% normal serum for 1 hr. They were then reacted with primary antibodies, including rabbit anti-cFos (1:2,500; Millipore, ABE457), goat anti-MCH (1:250; Santa Cruz, 14509), goat anti-orexin (1:250; Santa Cruz, 8070) or mouse anti-Lhx6 (1:250; Santa Cruz, 271433) for 48 hr (4°C). Following washes, sections were incubated in 1:500 dilution of AlexaFluor 488- or 647-conjugated secondary antibodies (Jackson Immunoresearch) for 2 hr. Sections were mounted, cover slipped with Prolong Gold (Molecular Probes, P36930), and cured overnight in the dark (4°C). A positive control experiment for the immunostaining was performed by identifying positive immunoreaction in other brain regions that have been known to contain the antigen. A negative control was performed by incubating sections

in the increasing dilutions of primary antibodies until immunoreaction disappeared in the absence of the antibody.

2.8 | Confocal microscopy and cell counting

ZEN 2010 software was utilized with a confocal laser scanning microscope (LSM 800; Zeiss), which was equipped with blue argon (488 nm), green helium neon (543 nm) and red helium neon (633 nm) lasers. In the SMART setup, "best signal" was chosen. To obtain high-resolution images, a specific frame size (i.e., x^*y = 1,024 × 1,024) at speed 4 was selected with an averaging process (n = 4). Double- or triple-labelled neurons were rechecked for genuine labelling using a single channel illumination. Optical section thickness was between 0.6 and 1.8 µm. Tile scan was selected to obtain a wider view; three in the LHA were taken for ORX or MCH neurons, whereas three in the ZI were taken for Lhx6+ cells. The counting tool in the Adobe Photoshop CS6 (64 Bit) was used; cells were considered labelled when they exhibited clear cytoplasmic (i.e., mCherry+, MCH or ORX) or nuclear (i.e., cFos+ or Lhx6+) morphology.

2.9 | Data analysis

The paired t test was employed to analyse the values in Table 1, because the data were obtained from the same individuals at the same time of the day and on different days. The Mann–Whitney U-test was employed to analyse the data shown in Table 2.

3 | RESULTS

The TRAP mice were used in this study to identify the neurons in the LHA and ZI activated during W and PS hypersomnia. The methodology allowed us to label neurons expressing cFos at two different time-points. The mCherry labelling (so-called TRAPing) was induced in activated neurons when 4-OHT was injected (Figure 1a). Neurons were labelled with cFos when they were activated just before perfusion. Three protocols were used: PSR-PSR, W-PSR and W-W (Figure 1b). Based on polysomnographic data (Table 1), the efficiency of 48-hr PS deprivation was assessed as a means of inducing PS hypersomnia (Figure 1c). Seven representative PSR animals were selected for analysis; the proportions of PS during the first 30-min period varied from 0% to 17.78% in the control condition, whereas they were between 24.17% and 53.06% during the PSR condition (Table 1). The amount of PS was significantly higher in PSR (Figure 1c, blue line) than in the control condition (Figure 1c, black line) during all four 30-min periods. Thus, 48-hr PS deprivation was efficient in inducing a significant PS hypersomnia during the subsequent 2-hr rebound period.

We compared the distribution of mCherry+ (or cFos+) ORX neurons in W-W versus W-PSR animals (Figure 2). In W-W animals (Figure 2B4), many ORX neurons were either cFos+ or mCherry+. A large number of cells were triple-labelled, exhibiting a white nucleus with violet cytoplasm. In W-PSR animals (Figure 2D4), mCherry+ ORX neurons representing cells activated during W were numerous, whereas cFos+ ORX cells were rare. Triple-labelled neurons were not observed in this case.

Quantitative analysis was performed to characterize the neurons activated in W-W and W-PSR conditions (Figure 3, the top row; Table 2, rows 3–10). In W-W mice, the average numbers of mCherry+ and cFos+ neurons in the LHA were 325 ± 93 (n = 3) and 405 ± 41 (n = 3), respectively. The average number of double-labelled (mCherry+ and cFos+) cells was 123 ± 22, which corresponds to approximately 37.8% of the mCherry+ cells and 30.4% of the cFos+ cells. In W-PSR mice, the average numbers of mCherry+ and cFos+ neurons were 281 ± 40 and 71 ± 22, respectively. On average, only three neurons were double-labelled, indicating that different groups of cells are activated during W and PSR. Based on the number of labelled cells (Figure 3, the top row), the proportions of labelled neuronal groups were analysed (Table 2, rows 3–10). In W-W animals, the average percentages of double-labelled (mCherry+ and ORX+) neurons over total mCherry+ cells and total ORX neurons were 31.1 ± 4.2% and 32.3 ± 5.0%, respectively. The values were in the same range in W-PSR animals. The percentages of cFos+ ORX neurons over total cFos+ cells and total ORX neurons in W-W animals were 30.7 ± 0.5% and 42.9 ± 4.3%, respectively. In contrast, in W-PSR mice, the percentages were 6.2 ± 0.9% and 1.6 ± 0.2%, respectively, indicating that ORX neurons are not activated during PSR. In line with this assumption, the average number of triple-labelled (mCherry+, cFos+ and ORX+) neurons was 57 ± 12 in W-W animals (Figure 3, the top row), but it was zero in the W-PSR mice. Impressively, the percentage of triple-labelled neurons in W-W mice constituted 19.6 ± 3.6% of all ORX neurons (Table 2).

We then determined whether the neurons activated during PSR correspond to MCH neurons. In a PSR-PSR animal, a large number of cFos+ (or mCherry+) MCH neurons were observed, but there were only a few triple-labelled MCH cells (Figure 4A–B4). In a W-PSR animal, however, a large proportion of MCH cells were cFos+, but there were few mCherry+ MCH cells (Figure 4C–D4), indicating that MCH neurons are activated during PSR but not during W.

Quantitative analysis was performed to compare the number of MCH neurons activated in PSR-PSR versus W-PSR mice (Figure 3, the second row; Table 2, rows 11–18). In PSR-PSR animals, the average numbers of mCherry+ and cFos+ neurons in the LHA were 369 ± 27 (n = 3) and 192 ± 64 (n = 3), respectively (Figure 3, the second row). The number of double-labelled (mCherry+ and cFos+) cells was 53 ± 11, which corresponds to 14.4% of the mCherry+ neurons and 27.6% of the cFos+ cells. In W-PSR animals, the numbers of mCherry+ and cFos+ neurons were 273 ± 29 and 197 ± 27, respectively. On average, only 10 neurons were double-labelled in W-PSR animals, indicating that different populations of neurons are activated during W and PSR. Based on the number of labelled cells (Figure 3, the second row), the proportions of labelled neuronal

groups were analysed (Table 2, rows 11–18). The average percentages of mCherry+ MCH cells over total mCherry+ neurons and total MCH cells in PSR-PSR animals were 5.7 ± 1.5% and 9.1 ± 2.7%, respectively. In contrast, these values were only 1.6 ± 0.3% and 2.0 ± 0.1% in W-PSR animals. Finally, the percentages of cFos+ MCH neurons over total cFos+ cells and total MCH neurons in PSR-PSR animals were 20.6 ± 4.8% and 16.6 ± 7.5%, respectively. These values were similar in W-PSR animals (i.e., 23.7 ± 1.2% and 21.9 ± 1.6%). An extremely limited number of triple-labelled cells was observed only in one PSR-PSR animal (Table 2, M1312).

We finally examined whether Lhx6+ neurons mainly localized in the ZI are activated during W or PS hypersomnia. The micrograph (Figure 5A–C4) shows a substantial number of triple-labelled, Lhx6+ neurons in a PSR-PSR animal. Because Lhx6 is a nuclear protein (like cFos), triple-labelled cells in the ventral ZI exhibited red (i.e., mCherry-labelled) cytoplasm with a white nucleus; many mCherry+ (or cFos+) Lhx6-immunoreactive neurons are also visible in the region. In a W-PSR animal, however, many cFos+ Lhx6 neurons are visible but only a few mCherry+ Lhx6 cells (Figure 5D–F4).

Quantitative analysis was performed to examine the activation of Lhx6+ neurons in PSR-PSR versus W-PSR animals (Figure 3, the bottom row; Table 2, rows 19–26). In PSR-PSR animals, the average numbers of mCherry+ and cFos+ neurons in the ZI were 193 ± 21 (n = 3) and 100 ± 27 (n = 3), respectively (Figure 3, the bottom row). The number of double-labelled (mCherry+ and cFos+) cells was 17 ± 2, which corresponds to 8.8% of the mCherry+ neurons and 17.0% of the cFos+ cells. In W-PSR animals, the average numbers of mCherry+ and cFos+ neurons were 218 ± 15 and 147 ± 51, respectively. On average, only nine neurons were double-labelled (i.e., mCherry+ and cFos+), indicating that different groups of neurons are activated during W and PSR. Based on the number of labelled cells (Figure 3, the bottom row), the proportions of labelled neuronal groups were analysed (Table 2, rows 19–26). The average percentages of mCherry+ Lhx6 neurons over total mCherry+ cells and total Lhx6+ neurons in PSR-PSR animals were 8.8 ± 2.3% and 4.6 ± 1.0%, respectively. These values were significantly (p < .05) higher than those seen in W-PSR animals (i.e., 2.1 ± 0.4% and 1.7 ± 0.4%), indicating that Lhx6+ neurons are activated during PSR rather than during W. In addition, the percentages of double-labelled (cFos+ and Lhx6+) neurons over total cFos+ cells and total Lhx6+ neurons were 24.6 ± 5.9% and 5.9 ± 0.7%, respectively. These values were in the same range as W-PSR animals (i.e., 23.0 ± 5.4% and 10.2 ± 1.0%). Altogether, these results indicate that a substantial proportion of the ZI neurons activated during PSR (but not during W) correspond to Lhx6+ neurons. In line with these results, the average percentage of triple-labelled neurons over total Lhx6+ cells was significantly (p < .05) larger in PSR-PSR than in W-PSR animals (Table 2, the last column).

4 | DISCUSSION

In the present study, we first report that a large proportion of neurons labelled with mCherry during W (37.8%) or PSR (14.4%) express cFos when the animals are re-exposed to the same conditions (i.e., W-W or PSR-PSR) just before perfusion, whereas the proportions are much smaller (i.e., 1.1% and 3.7%) when the animals are exposed to two different conditions (i.e., W-PSR). In addition, we found that ORX neurons known to be specifically active during W (Lee, Hassani, & Jones, 2005) express cFos during W but not during PSR, whereas those expressing MCH known to be specifically active during PSR (Gao, 2009; Peever & Fuller, 2016; Verret et al., 2003) are mCherry+ during PSR and not during W. These results first indicate that a large proportion of the neurons expressing mCherry express cFos when the animals are re-exposed to the same condition, validating the TRAP methodology for studying neurons activated during W or PSR. In addition, we observed that 8.8% of ZI neurons labelled with mCherry during PSR expressed Lhx6, in contrast to the W condition, in which only 2.1% of the mCherry+ cells expressed Lhx6. These results indicate that Lhx6+ neurons are specifically activated during PSR. These values are even higher than those seen with MCH, suggesting that Lhx6+ neurons might be specifically active during PS, like the MCH cells.

The TRAP method has never been utilized to study neurons activated during PS hypersomnia and W. We showed here that a large percentage of the neurons labelled with mCherry are cFos+ in W-W and PSR-PSR but not in W-PSR conditions. Further, we showed that a large percentage of the mCherry+ and cFos+ cells labelled after the W condition express ORX and not MCH, indicating that mCherry is expressed in W-active neurons, and thus validating the specificity of the staining obtained. Further, we confirmed the specificity for activated neurons of the mCherry labelling obtained after PSR because a large number of the mCherry+ neurons expressed MCH. In addition, the fact that nearly no ORX neurons were labelled in the PSR condition indicates that although there are some W episodes during PSR, it is not sufficient to induce mCherry or cFos staining.

In summary, our results clearly indicate that the TRAP method can be used to study neurons activated during PSR and W, introducing a powerful new method to study such neurons. This is in line with a recent study using TRAP mice to identify a previously unknown population of glutamatergic neurons involved in the generation of SWS (Zhang et al., 2019). Our study opens the possibility to fully characterize PS-activated neurons across the brain, by combining the TRAP methodology with mRNAs sequencing, "in vitro" recordings, and optogenetic and chemogenetic approaches. Furthermore, we demonstrated for the first time that Lhx6+ neurons of the ZI were activated during PSR like the MCH neurons, and not during W. We previously showed that most of the neurons expressing cFos in the ZI during PSR express GAD67 (Sapin et al., 2010). It has been recently shown that Lhx6+ neurons of the ZI express vGAT and GAD67 and are distinct from MCH and ORX neurons (Liu et al., 2017; Mickelsen et al., 2019). It is therefore likely that the Lhx6+ neurons in the ZI constitute a sub-population of the PS-activated GABAergic neurons.

In a previous report, Liu et al. (2017) demonstrated that cFos expression is increased in Lhx6+ neurons at light onset and after

6 hr of total sleep deprivation, with or without 1 hr of sleep recovery. From these results, they concluded that Lhx6+ neurons are activated by sleep pressure. Although this is not directly comparable to our results, we did find that cFos expression was strongly increased in Lhx6+ neurons after 2 hr of PSR and not after 2 hr of W. Our results therefore indicate that these neurons are more active during PSR than during W. Unit recordings of these neurons are eventually needed to confirm this hypothesis. Liu et al. (2017) further showed that the loss of Lhx6+ neurons (which was directly induced by gene deletion from the developing diencephalon) caused an increase in W and a reduction of SWS and PS, with a relative decrease of PS greater than that of SWS. Likewise, clozapine N oxide (CNO) injection after transfecting Lhx6+ neurons with excitatory designer receptors exclusively activated by designer drugs (DREADDS) induced an increase in PS and to a minor extent in SWS, whereas inhibition of Lhx6+ cells transfected with inhibitory DREADDS reduced sleep (PS in particular). They further showed that Lhx6+ cells project to the ORX cells as well as monoaminergic W-active neurons and are likely to induce sleep by inhibiting them. These observations are similar to what has been reported for the activation or inhibition of MCH neurons (Jego et al., 2013; Varin et al., 2018). Altogether, these and our results suggest that like MCH neurons, Lhx6+ cells in the ZI might contribute to PS.

In addition to these two populations of neurons, other neurons in the LHA and ZI express cFos following PSR; thus, further experiments are needed to identify these neurons and characterize their specific functions. In conclusion, the present findings demonstrate that TRAP methodology combined with our automatic PS-deprivation system constitutes a promising new strategy to identify various types of neurons involved in PS.

ACKNOWLEDGEMENTS

This paper was written as part of Konkuk University's research support programme for its faculty (Hyun-Sook Lee) on sabbatical leave in 2018. This work was supported by the Centre National de la Recherche Scientifique, Université de Lyon and Université Lyon 1. RY was funded by the JSPS Overseas Challenge Program for Young Researchers from The Japan Society for the Promotion of Science and a Postdoctoral Fellowship from the Uehara Memorial Foundation, French Embassy in Japan.

CONFLICT OF INTEREST

No conflicts of interest declared.

AUTHOR CONTRIBUTIONS

PHL, PF and LAD designed the experiment. RY, DW and SA performed physiological recordings. HSL performed anatomical works with data analysis. HSL and PHL wrote the manuscript.

ORCID

Patrice Fort https://orcid.org/0000-0003-1211-8631
Pierre-Hervé Luppi https://orcid.org/0000-0002-0503-423X

REFERENCES

Allen, W. E., DeNardo, L. A., Chen, M. Z., Liu, C. D., Loh, K. M., Fenno, L. E., … Luo, L. (2017). Thirst-associated preoptic neurons encode an aversive motivational drive. *Science*, *357*, 1149–1155. https://doi.org/10.1126/science.aan6747

Arthaud, S., Varin, C., Gay, N., Libourel, P.-A., Chauveau, F., Fort, P., … Peyron, C. (2015). Paradoxical (REM) sleep deprivation in mice using the small-platforms-over-water method: Polysomnographic analyses and melanin-concentrating hormone and hypocretin/orexin neuronal activation before, during and after deprivation. *The Journal of Sleep Research*, *24*, 309–319. https://doi.org/10.1111/jsr.12269

Blanco-Centurion, C., Luo, S., Spergel, D. J., Vidal-Ortiz, A., Oprisen, S., Van den Pol, A. N., … Shiromani, P. J. (2019). Dynamic network activation of hypothalamic MCH neurons in REM sleep and exploratory behavior. *The Journal of Neuroscience*, *39*, 4986–4998. https://doi.org/10.1523/JNEUROSCI.0305-19.2019

Brown, R. E., Yang, C., Winston, S., Anderson-Chernisof, M., McNally, J. M., & McKenna, J. T. (2017). Investigation of the developmental origin of forebrain GABAergic neurons involved in sleep-wake control using a fate-mapping approach. *Sleep*, *40*(suppl. 1), A17. https://doi.org/10.1093/sleepj/zsx050.042

DeNardo, L. A., Liu, C. D., Allen, W. E., Adams, E. L., Friedmann, D., Fu, L., … Luo, L. (2019). Temporal evolution of cortical ensembles promoting remote memory retrieval. *Nature Neuroscience*, *22*, 460–469. https://doi.org/10.1038/s41593-018-0318-7

DeNardo, L. A., & Luo, L. (2017). Genetic strategies to access activated neurons. *Current Opinion in Neurobiology*, *45*, 121–129. https://doi.org/10.1016/j.conb.2017.05.014g/10.1038/s41593-018-0318-7

Gao, X.-B. (2009). Electrophysiological effects of MCH on neurons in the hypothalamus. *Peptides*, *30*, 2025–2030. https://doi.org/10.1016/j.peptides.2009.05.006

Girasole, A. E., Lum, M. Y., Nathaniel, D., Bair-Marshall, C. J., Guenthner, C. J., Luo, L., … Nelson, A. B. (2018). A subpopulation of striatal neurons mediates levodopa-induced dyskinesia. *Neuron*, *97*, 787–795. https://doi.org/10.1016/j.neuron.2018.01.017

Guenthner, C. J., Miyamichi, K., Yang, H. H., Heller, H. C., & Luo, L. (2013). Permanent genetic access to transiently active neurons via TRAP: Targeted recombination in active populations. *Neuron*, *78*, 773–784. https://doi.org/10.1016/j.neuron.2013.03.025

Hassani, O. K., Lee, M. G., & Jones, B. E. (2009). Melanin-concentrating hormone neurons discharge in a reciprocal manner to orexin neurons across the sleep-wake cycle. *Proceedings of the National Academy of Sciences of the United States of America*, *106*, 2418–2422. https://doi.org/10.1073/pnas.0811400106

Herrera, C. G., Cadavieco, M. C., Jego, S., Ponomarenko, A., Korotkova, T., & Adamantidis, A. (2016). Hypothalamic feed-forward inhibition of thalamocortical network controls arousal and consciousness. *Nature Neuroscience*, *19*, 290–298. https://doi.org/10.1038/nn.4209

Jego, S., Glasgow, S. D., Herrera, C. G., Ekstrand, M., Reed, S. J., Boyce, R., … Adamantis, A. R. (2013). Optogenetic identification of a rapid eye movement sleep modulatory circuit in the hypothalamus. *Nature Neuroscience*, *16*, 1637–1643. https://doi.org/10.1038/nn.3522

Lee, M. G., Hassani, O. K., & Jones, B. E. (2005). Discharge of identified orexin/hypocretin neurons across the sleep-waking cycle. *The Journal of Neuroscience*, *25*, 6716–6720. https://doi.org/10.1523/JNEUROSCI.1887-05.2005

Libourel, P. A., Corneyllie, A., Luppi, P. H., Chouvet, G., & Gervasoni, D. (2015). Unsupervised online classifier in sleep scoring for sleep deprivation studies. *Sleep*, *38*, 815–828. https://doi.org/10.5665/sleep.4682

Liu, K., Kim, J., Kim, D. W., Zhang, Y. S., Bao, H., Denaxa, M., … Blackshaw, S. (2017). Lhx6-positive GABA-releasing neurons of the zona incerta promote sleep. *Nature*, *548*, 582–587. https://doi.org/10.1038/nature23663

Mickelsen, L. E., Bolisetty, M., Chimileski, B. R., Fujita, A., Beltrami, E. J., Costanzo, J. T., … Jackson, A. C. (2019). Single-cell transcriptomic analysis of the lateral hypothalamic area reveals molecularly distinct populations of inhibitory and excitatory neurons. *Nature Neuroscience*, *22*, 642–656. https://doi.org/10.1038/s41593-019-0349-8

Peever, J., & Fuller, P. M. (2016). The biology of REM sleep. *Current Biology*, *26*, R34–R35. https://doi.org/10.1016/j.cub.2015.11.011

Renouard, L., Billwiller, F., Ogawa, K., Clément, O., Camargo, N., Abdelkarim, M., … Luppi, P. H. (2015). The supramammillary nucleus and the claustrum activate the cortex during REM sleep. *Science Advances*, *1*, e1400177. https://doi.org/10.1126/sciadv.1400177

Sapin, E., Berod, A., Léger, L., & Herman, P. A. (2010). A very large number of GABAergic neurons are activated in the tuberal hypothalamus during paradoxical (REM) sleep hypersomnia. *PLoS One*, *5*, e11766. https://doi.org/10.1073/pnas.0811400106

Sapin, E., Lapray, D., Bérod, A., Goutagny, R., Léger, L., Ravassard, P., … Luppi, P.-H. (2009). Localization of the brainstem GABAergic neurons controlling paradoxical (REM) sleep. *PLoS One*, *4*, e4272. https://doi.org/10.1371/journal.pone.0004272

Tasaka, G., Guenthner, C. J., Shalev, A., Gilday, O., Luo, L., & Mizrahi, A. (2018). Genetic tagging of active neurons in auditory cortex reveals maternal plasticity of coding ultrasonic vocalizations. *Nature Communications*, *9*, 871–884. https://doi.org/10.1038/s41467-018-03183-2

Varin, C., Luppi, P.-H., & Fort, P. (2018). Melanin-concentrating hormone-expressing neurons adjust slow-wave sleep dynamics to catalyze paradoxical (REM) sleep. *Sleep*, *41*(6), 1–12. https://doi.org/10.1093/sleep/zsy068

Verret, L., Gautagny, R., Fort, P., Cagnon, L., Salvert, D., Léger, L., … Luppi, P.-H. (2003). A role of melanin-concentrating hormone producing neurons in the central regulation of paradoxical sleep. *BMC Neuroscience*, *4*, 19. https://doi.org/10.1186/1471-2202-4-19

Zhang, Z., Zhong, P., Hu, F., Barger, Z., Ren, Y., Ding, X., … Dan, Y. (2019). An excitatory circuit in the perioculomotor midbrain for non-REM sleep control. *Cell*, *177*, 1293–1307. https://doi.org/10.1016/j.cell.2019.03.041

How to cite this article: Lee H-S, Yamazaki R, Wang D, et al. Targeted recombination in active populations as a new mouse genetic model to study sleep-active neuronal populations: Demonstration that Lhx6+ neurons in the ventral zona incerta are activated during paradoxical sleep hypersomnia. *J Sleep Res*. 2020;00:e12976. https://doi.org/10.1111/jsr.12976